IEEE Access
Multidisciplinary | Rapid Review | Open Access Journal

Received January 2, 2021, accepted January 21, 2021, date of publication February 4, 2021, date of current version February 17, 2021.

Digital Object Identifier 10.1109/ACCESS.2021.3057123

Rooted Tree Optimization for the Backstepping Power Control of a Doubly Fed Induction Generator Wind Turbine: dSPACE Implementation

BADRE BOSSOUFI[1], (Graduate Student Member, IEEE), MOHAMMED KARIM[1], MOHAMMED TAOUSSI[1], HALA ALAMI AROUSSI[2], MANALE BOUDERBALA[1], OLIVIER DEBLECKER[3], SAAD MOTAHHIR[4], (Member, IEEE), ANAND NAYYAR[5,6], AND MOHAMMED A. ALZAIN[7]

[1]LIMAS Laboratory, Faculty of Sciences, Sidi Mohamed Ben Abdellah University, Fez 30000, Morocco
[2]LGEM Laboratory, Higher School of Technology, Mohammed First University, Oujda 60040, Morocco
[3]EPEU Unit, Polytech of Mons, 7000 Mons, Belgium
[4]Engineering, Systems, and Applications Laboratory, ENSA, Sidi Mohamed Ben Abdellah University, Fez 30000, Morocco
[5]Graduate School, Duy Tan University, Da Nang 550000, Vietnam
[6]Faculty of Information Technology, Duy Tan University, Da Nang 550000, Vietnam
[7]Department of Information Technology, College of Computers and Information Technology, Taif University,Taif 21944, Saudi Arabia

Corresponding authors: Badre Bossoufi (badre.bossoufi@usmba.ac.ma) and Anand Nayyar (anandnayyar@duytan.edu.vn)

This work was supported by Taif University Researchers Supporting Project, Taif University, Saudi Arabia, under Grant TURSP-2020/98.

ABSTRACT With the development of wind power generation in recent years, several studies have dealt with the active and reactive power control of wind power systems, along with the quality of energy produced and the connection to distribution networks. In this context, this research proposes a new contribution to the field. The major objective of this work is the development of a nonlinear adaptive backstepping control technique applied to a DFIG based wind system and an optimization technique that uses the rooted tree optimization (RTO) algorithm. The backstepping control strategy is based on the Lyapunov nonlinear technique to guarantee the stability of the system. It is applied to the two converters (i.e., machine and network sides) and subsequently improved with estimators to make the proposed system robust to parametric variation. The RTO technique is based on monitoring the behavior of the underlying foundation of trees in search of underground water in accordance with the level of underground control. The solution proposed for the control is validated using two methods: (1) a simulation on MATLAB/Simulink to test the continuation of the reference (real wind speed) and the robustness of the system and (2) a real-time implementation on a dSPACE-DS1104 board connected to an experimental bench in a laboratory. Simulation and experimental results highlight the validation of the proposed model with better performance compared with other control techniques, such as sliding mode control, direct power control, and field-oriented control.

INDEX TERMS Wind turbine, energy, backstepping control, adaptive control, MATLAB/simulink, wind turbine, dSPACE.

f_r, f_s	Frequency at the rotor and stator
Ω_t	Turbine speed
R_s, R_r	Resistance of the stator/rotor
R_f, L_f	Resistance and inductance of a phase of the filter
L_r, L_s	Inductance of the stator/rotor
P_s, P_r, P_g	Active power at the stator, rotor, and grid
Q_s, Q_r, Q_g	Reactive power to the stator, rotor, and network
$P_{mec}, P_{res}, P_{elec}$	Mechanical, network, and electrical power
P_{ins}, P_{ext}	Recoverable wind and theoretical power
T_{em}, C_{em}	Electromagnetic torque

The associate editor coordinating the review of this manuscript and approving it for publication was Xiaodong Liang.

$V_{r(a,b,c)}$, $V_{s(A,B,C)}$	Rotor and stator voltages
$i_{r(a,b,c)}$, $i_{s(A,B,C)}$	Rotor and stator currents
$\psi_{r(a,b,c)}$, $\psi_{s(A,B,C)}$	Rotor and stator flux
(v_{sd}, v_{sq}), (i_{sd}, i_{sq})	d/q stator voltages and currents
(v_{rd}, v_{rq}), (i_{rd}, i_{rq})	d/q rotor voltages and currents
(v_{gd}, v_{gq}), (i_{gd}, i_{gq})	Grid voltages and currents
(v_{td}, v_{tq}), (i_{td}, i_{tq})	Voltages and currents at the RL filter

I. INTRODUCTION

Renewable energy forms have become the most coveted energy sources at present because they ensure autonomy for all nations [1]. Created from inexhaustible resources, these energy forms do not require storage. Thus, their utilization guarantees the continuity of production without worrying about fluctuations in the prices of raw materials in international energy markets [2].

Sustainable power sources are the most reasonable approach for improving decentralized energy supply. These resources are particularly significant for certain developing nations and developed countries. The utilization of renewable energy sources makes enhancing the common assets of regions conceivable by creating new industries and transport and promoting urbanization. This practice also controls the exploitation and reduces the consumption of fuel [3]. Moreover, it decreases the cost of energy production compared with classical energy sources.

At present, renewable sources provide an impressive potential for a financial, modern, and social turn of events. The rapid development of global environment-friendly power markets involves every sector in different project openings. Rivalry is all-inclusive. The technological advancement in this field will increase the use of renewable energy sources, which will reduce the cost of energy and pollution.

The International Energy Agency forecasts that by 2040, renewable energy sources will cover 58% of electricity supply, 22% of inexhaustible warmth and cold generation, and 20% of transport if we intend to keep the temperature on the Earth's surface below 2 °C. Sustainable power sources will cover nearly 60% of developed installations until 2040. Between 2016 and 2040, over 4,000 GW of renewable energy must be operated, representing four times the thermal capacity generated in the same period. Numerous reasons motivate this development: decrease in costs, dispersion of innovations on a worldwide scale, economic and international pressures associated with the excessive use of hydrocarbons, and determination to respect the commitments made in the Paris Agreement.

The quality of energy produced from a wind power system must follow international standards, i.e., a total harmonic distortion (THD) rate of less than 5% [1]–[17].

The objectives of the current work are as follows [4]–[20]:

- To decrease the expenses related to the production of electrical energy by solar and wind power plants and improve the quality of electrical energy supplied by these power plants, and
- To propose logical solutions for the implementation of inexhaustible sources in smart grids that require reliable production systems.

Achieving these objectives will promote the enhancement of electrical energy quality produced from sustainable sources [5]. This improvement in production will affect the selling price of this type of energy. Thus, we have to consider the important constituent that will assure such progress, namely, control strategies [6], [21].

The reduction in electrical energy cost presupposes the following:

- The increase in the reliability and robustness of wind power plants,
- The manufacture of lighter wind turbines (WTs) that exhibit high performance,
- The increase in energy efficiency, and
- The robustness of the designed control algorithms.

Decentralized energy sources have several drawbacks, such as no voltage adjustment, no frequency regulation, and the impossibility of operating on an island. Energy production from renewable energy sources is difficult to predict and fluctuates considerably. Thus, integrating decentralized units into an electrical grid will certainly cause problems as mentioned previously [5], [7]–[22].

This study sets an objective, namely, the application of a nonlinear adaptive backstepping command in real time on a wind energy conversion system (WECS)-doubly-fed induction generator (DFIG) controlled by power converters (grid and generator sides). Moreover, the primary objective is to command the wind system via a DS1104 R&D controller board under variable wind reference.

The contributions of this research are as follows:

- Conduct a nonlinear modeling of a wind power system,
- Ensure and optimize the operation of a wind power system through a nonlinear model of the system that uses a nonlinear control technique,
- Develop a robust control technique with estimators,
- Provide control optimization based on the rooted tree optimization (RTO) algorithm, and
- Experimentally implement and validate the proposed model on a benchmark based on a 1.5 kW DFIG and a dSPACE DS1104 card.

This paper is divided into five sections. *Section II* highlights the literature review of various papers being considered for study and conduct research to define the problem and identify technical gaps.

II. LITERATURE REVIEW

On the basis of several studies in the literature that developed classical techniques, such as backstepping control, sliding mode control (SMC), field-oriented control (FOC), and predictive control, we design a new robust and optimal control strategy that can overcome the disadvantages of these types of control. We present some examples in this section.

In *Zhang et al. (2014)* [7], direct torque control (DTC) command based on a support vector machine was applied to

a permanent magnet synchronous generator (PMSG)-based wind power system. Then, DTC command was combined with an observer in sliding mode that used a relatively low sampling frequency to estimate rotor position and stator flux connection.

Beltran et al. (2012) [8] presented the application of the maximum power point tracking (MPPT) command and SMC to a wind power system based on DFIG. Their research aimed to control the desired electromagnetic torque by using current control. Moreover, estimates were used to define the references that caused certain inaccuracies, leading mostly to nonoptimal power extraction.

Yang et al. (2018) [9] implemented SMC on DFIG. The obtained results were inefficient in terms of robustness and set-point follow-up (chattering phenomenon).

Benbouzid et al. (2010) [11] presented a control that led to the production of electricity under variable speed for WT systems. Systems have two operating zones that depend on WT tip speed ratio. A high-order sliding mode strategy was suggested to guarantee stability in the two operating zones and achieve the optimal performances.

In accordance with the literature review, the majority of control algorithms, either for DFIG-based or PMSG-based wind systems, experience problems in terms of robustness and real-time implantation. Our contribution in the current work is to confirm the performance of an adaptive model by implementing and validating it on a test bench based on a dSPACE card.

III. WIND POWER SYSTEM MODEL

The development of the backstepping control for wind power systems requires a specific model (nonlinear) of the machine. Hence, the analytical model of DFIG is essential. The model adopted must be close to reality and nonlinear to facilitate implementation [12]. The structure of the wind power system is illustrated in Fig. 1 [5]–[23].

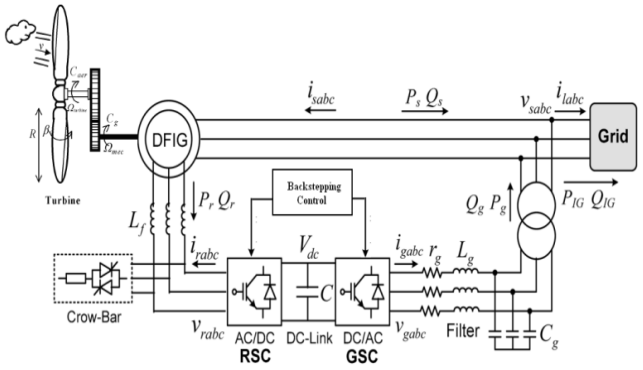

FIGURE 1. Structure of the wind power system.

The objective of this section is to model the WECS-DFIG, particularly the kinetic (turbine), mechanical (shaft and gearbox), and electrical [generator, load-side converter, rotor-side converter (RSC), DC bus, and filter] parts.

The structure of the entire system is shown in Figure 1.

A. WT MODEL

The turbine model is deduced from the following system [1]:

$$P_{incident} = \frac{1}{2}.\rho.A.v^3, \tag{1}$$

$$P_{extracted} = \frac{1}{2}.\rho.A.C_p(\lambda,\beta).v^3, \tag{2}$$

with

$$\lambda = \frac{\Omega_t.R}{v}, \tag{3}$$

$$J = \frac{J_{tur}}{G^2} + J_g, \tag{4}$$

$$J\frac{d\Omega_{mec}}{dt} = C_{mec} = C_{ar} - C_{em} - f.\Omega_{mec}. \tag{5}$$

B. DFIG MODEL

Many researchers have represented the DFIG model in reference frame *dq* by using four types of equations [13], [17].

1) ELECTRICAL EQUATIONS

The voltages in the reference frame *dq* yields

$$\begin{cases} V_{sd} = R_s.I_{sd} + \dfrac{d\phi_{sd}}{dt} - \omega_s.\phi_{sq} \\ V_{sq} = R_s.I_{sq} + \dfrac{d\phi_{sq}}{dt} + \omega_s.\phi_{sd} \\ V_{rd} = R_r.I_{rd} + \dfrac{d\phi_{rd}}{dt} - \omega_r.\phi_{rq} \\ V_{rq} = R_r.I_{rq} + \dfrac{d\phi_{rq}}{dt} + \omega_r.\phi_{rd}. \end{cases} \tag{6}$$

2) FLUX EQUATIONS

The flux (stator and rotor) is connected to the current (stator and rotor) by the following expressions:

$$\omega_r = \omega_s - p.\Omega$$

$$\begin{cases} \varphi_{ds} = L_s.i_{ds} + M.i_{dr} \\ \varphi_{qs} = L_s.i_{qs} + M.i_{qr} \\ \varphi_{dr} = L_r.i_{dr} + M.i_{ds} \\ \varphi_{qr} = L_r.i_{qr} + M.i_{qs}. \end{cases}$$

$$L_s = l_s - M_s, \quad L_r = l_r - M_r \tag{7}$$

3) ELECTROMAGNETIC TORQUE

The electromagnetic torque is expressed as [1]–[24]

$$C_{em} = p\left(\phi_{ds}i_{qs} - \phi_{qs}i_{ds}\right). \tag{8}$$

4) ACTIVE AND REACTIVE POWERS

The stator and rotor powers (active and reactive) of DFIG are written as [1]

$$\begin{cases} P_s = v_{ds}.i_{ds} + v_{qs}.i_{qs} \\ Q_s = v_{qs}.i_{ds} - v_{ds}.i_{qs} \\ P_r = v_{dr}.i_{dr} + v_{qr}.i_{qr} \\ Q_r = v_{qr}.i_{dr} - v_{dr}.i_{qr}. \end{cases} \tag{9}$$

IV. BACKSTEPPING CONTROL TECHNIQUE

A. RSC CONTROL

In this section, we propose a control model, namely, the nonlinear backstepping technique based on the Lyapunov function; this technique is adaptive with a machine parameter estimator [1], [14].

The rotor-side control aims to ensure the stability of the active and reactive powers. First, we define the errors as follows:

$$e_{P_s} = P_{s\_ref} - P_s, \tag{10}$$
$$e_{Q_s} = Q_{s\_ref} - Q_s. \tag{11}$$

Then, we express the Lyapunov function as [13], [14]

$$V_1 = \frac{1}{2}e_{P_s}^2, \tag{12}$$
$$V_2 = \frac{1}{2}(e_{Vdc}^2 + e_{Pq}^2 + e_{Qs}^2). \tag{13}$$

To ensure that the stability of the system is realized, the negativity of the derivative of the Lyapunov functions (V_1 and V_2) must be guaranteed. To achieve this goal, we introduce a positive constant into the derivative (V_1 and V_2) as follows:

$$\dot{V}_1 = -k_{Ps}e_{Ps}^2 \leq 0, \tag{14}$$
$$\dot{V}_2 = -K_{Vdc}e_{Vdc}^2 - K_{Ps}e_{Pq}^2 - K_{Qs}e_{Qs}^2 \leq 0. \tag{15}$$

After calculation, we obtain the following vectors, (16), as shown at the bottom of the page.

Moreover, we find the virtual reference input as (17), shown at the bottom of the page.

B. GRID-SIDE CONVERTER CONTROL

Control in the grid side ensures the stability of the amplitude voltage of the DC link and maintains the unit power factor [5], [10]–[14]. To achieve these objectives, we express the errors [5]–[28] as follows:

$$e_{V_{dc}} = V_{dc\_ref} - V_{dc}, \tag{18}$$
$$\begin{cases} e_{P_g} = P_{g\_ref} - P_g \\ e_{Q_g} = Q_{g\_ref} - Q_g, \end{cases} \tag{19}$$
$$V_1 = \frac{1}{2}e_{V_{dc}}^2, \tag{20}$$
$$V_2 = \frac{1}{2}\left(e_{V_{dc}}^2 + e_{P_g}^2 + e_{Q_g}^2\right). \tag{21}$$

As mentioned previously, the derivative of the Lyapunov functions (V_1, V_2) must be negative. Hence, we introduce a positive constant into the derivative (V_1 and V_2) as follows:

$$\dot{V}_1 = -K_{Vdc}e_{Vdc}^2 \leq 0, \tag{22}$$
$$\dot{V}_2 = -K_{Vdc}e_{Vdc}^2 - K_{Ps}e_{Pq}^2 - K_{Qs}e_{Qs}^2 \leq 0. \tag{23}$$

After calculation, we obtain the following vectors:

$$\begin{cases} v_{gd} = \dfrac{L_r}{\sqrt{\frac{3}{2}\hat{v}}}\left(K_{Ps}e_{Ps} + \dot{P}_{s-ref} + \dfrac{R_r}{L_r}P_s + \omega_s Q_s - \dfrac{1}{L_r}\left(v_{gd}^2 + v_{gq}^2\right)\right), \\ v_{gq} = \dfrac{L_r}{\sqrt{\frac{3}{2}\hat{v}}}\left(K_{Qs}e_{Qs} + \dot{Q}_{s-ref} + \dfrac{R_r}{L_r}Q_s + \omega_s P_s\right). \end{cases} \tag{24}$$

Moreover, we find the virtual reference input:

$$\begin{cases} P_{g\_ref} = P_g \\ v_{s\_ref} = \dfrac{P_{g\_ref}}{C.k_{v_{dc}}.e_{v_{dc}}} - P_r. \end{cases} \tag{25}$$

C. DFIG PARAMETER ESTIMATION

To approximate reality, we use observers to estimate the machine parameters and load torque, which, in turn, will support the development of the real model of the machine. The robustness of the control to parameter variations and measurement noise will be improved by developing such model. Subsequently, to design the adaptive nonlinear backstepping control, we replace the vectors of the real parameters of DFIG with their estimates. The expressions of the powers will be [5]

$$\begin{cases} \dot{e}_{Ps} = \dot{P}_{s-ref} + \hat{a}_2 P_s + \begin{pmatrix} \hat{a}_3\left(v_{sd}\varphi_{sd} + v_{sq}\varphi_{sq}\right) \\ +\hat{a}_4\left(-v_{sd}v_{sq} + v_{rd}v_{rq}\right) \\ +\hat{a}_5 V_s^2 - Q_s\omega_s \end{pmatrix}, \\ \dot{e}_{Qs} = \dot{Q}_{s-ref}\left(\hat{a}_2 Q_s + \begin{matrix} \hat{a}_3\left(v_{sd}\varphi_{sd} + v_{sq}\varphi_{sq}\right) \\ +\hat{a}_4\left(-v_{rd}+v_{rq}\right)v_{sd} - Q_s\omega_s \end{matrix}\right), \end{cases} \tag{26}$$

$$\hat{a}_2 = \left(\frac{\hat{R}_s.\hat{L}_r + \hat{R}_r.\hat{L}_s}{\hat{\sigma}.\hat{L}_s.\hat{L}_r}\right) \quad \hat{a}_3 = \left(\frac{3.\left(\hat{R}_r + \omega_r.\hat{L}_r\right)}{2.\hat{\sigma}.\hat{L}_s.\hat{L}_r}\right)$$
$$\hat{a}_4 = \left(\frac{3.M}{2.\hat{\sigma}.\hat{L}_s.\hat{L}_r}\right) \quad \hat{a}_5 = \left(\frac{3}{2.\hat{\sigma}.\hat{L}_s}\right). \tag{27}$$

$$\begin{cases} v_{rd} = \dfrac{1}{v_{sd}M}\left(\begin{matrix}\left(\frac{2\sigma L_s L_r}{3}\right)\left(K_{Ps}e_{Ps} + \dot{P}_{s-ref} - \omega_s Q_s\right) \\ \frac{2}{3}\left(R_s L_r + R_r L_s\right)P_s + \left(R_r + \omega_r L_r\right)\left(v_{sd}\varphi_{sd} + v_{sq}\varphi_{sq}\right) + L_r V_s^2\end{matrix}\right), \\ v_{rq} = -\dfrac{1}{v_{sd}M}\left(\begin{matrix}\left(\frac{2\sigma L_s L_r}{3}\right)\left(K_{Qs}e_{Qs} + \dot{Q}_{s-ref} - \omega_s P_s\right) \\ \frac{2}{3}\left(R_s L_r + R_r L_s\right)Qs + \left(R_r + \omega_r L_r\right)\left(v_{sd}\varphi_{sd} + v_{sq}\varphi_{sq}\right)\end{matrix}\right). \end{cases} \tag{16}$$

$$Q_{s\_ref} = Q_s \left\{ P_{s\_ref} = \frac{3}{2\left(R_s.L_r + R_r.L_s\right)}\left(\begin{matrix}\left(\frac{2.\sigma.L_s.L_r}{3}\right).\left(-k_{P_s}.e_{P_s} + \omega_s.Q_{s\_ref}\right) \\ -\left(\begin{matrix}\left(R_r + \omega_r.L_r\right).\left(v_{sd}.\psi_{sd} + v_{sq}.\psi_{sq}\right) \\ -M.\left(-v_{sd}.v_{rd} + v_{sq}.v_{rq}\right) + L_r.V_s^2\end{matrix}\right)\end{matrix}\right) \right. . \tag{17}$$

In the current work, we focus on the variations of parameters Rs, Rr, Ls, Lr, and σ. Nevertheless, estimating M is easy. Similarly, if Ls and Lr vary, then M also varies. Thereafter, a new Lyapunov function (V_2) is defined using gain adaptation as follows:

$$V_2 = \frac{1}{2}\left(e_\Omega^2 + e_{P_s}^2 + e_{Q_s}^2 + \frac{\tilde{C}_m^2}{\gamma_m} + \frac{\tilde{a}_1^2}{\gamma_1} + \frac{\tilde{a}_2^2}{\gamma_2} + \frac{\tilde{a}_3^2}{\gamma_3} + \frac{\tilde{a}_4^2}{\gamma_4} + \frac{\tilde{a}_5^2}{\gamma_5}\right). \tag{28}$$

We maintain the derivative of Equation (28) as zero to guarantee system stability. On the basis of the calculation procedure, we recommend the following control laws (V_{rd} and V_{rq}) :

$$\begin{cases} v_{rd} = \dfrac{1}{\hat{a}_4 v_{sd}}\begin{pmatrix} K_{Ps}e_{Ps} + \dot{P}_{s-ref} + \hat{a}_2 P_s - \omega_s Q_s \\ +\hat{a}_3\left(v_{sd}\varphi_{sd} + v_{sq}\varphi_{sq}\right) + \hat{a}_5 V_s^2 \end{pmatrix} + \dfrac{v_{sq}}{v_{sd}} v_{rq} \\ v_{rq} = \dfrac{1}{\hat{a}_4 v_{sd}}\begin{pmatrix} -K_{Qs}e_{Qs} + \dot{Q}_{s-ref} - \hat{a}_2 Q_s - \omega_s P_s \\ -\hat{a}_3\left(v_{sd}\varphi_{sd} + v_{sq}\varphi_{sq}\right) \end{pmatrix} + v_{rd}. \end{cases} \tag{29}$$

From Equation (29), we estimate the adaptation expressions of the DFIG parameters as follows.

1) STATOR AND ROTOR RESISTANCES

$$\begin{cases} \tilde{R}_r = \int \dot{\tilde{R}}_r = \int \dfrac{2\dot{\tilde{\sigma}}\dot{\tilde{L}}_s\dot{\tilde{L}}_r\dot{\tilde{a}}_3}{3} - \omega_r\dot{\tilde{L}}_r \\ = \dfrac{2}{3}\int \dot{\tilde{\sigma}}\dot{\tilde{L}}_s\dot{\tilde{L}}_r - \gamma_3\left(v_{sd}\varphi_{sd} + v_{sq}\varphi_{sq}\right)\left(e_{Ps} + e_{Qs}\right) - \omega_r\dot{\tilde{L}}_r, \\ \tilde{R}_s = \int \dot{\tilde{R}}_s = \int \dfrac{\dot{\tilde{\sigma}}\dot{\tilde{L}}_s\dot{\tilde{L}}_r\dot{\tilde{a}}_2\dot{\tilde{R}}_r\dot{\tilde{L}}_s}{\dot{\tilde{L}}_r} \\ = \int \gamma_2\dot{\tilde{\sigma}}\dot{\tilde{L}}_s(-e_{Ps}P_s - e_{Qs}Q_s) - \dfrac{\dot{\tilde{L}}_s}{\dot{\tilde{L}}_r}\dot{\tilde{R}}_r. \end{cases} \tag{30}$$

2) STATOR AND ROTOR INDUCTANCES

See (31), as shown at the bottom of the page.

V. RTO ALGORITHM

The basic development for trees is related to a very rooted structure. From this point of view, underground root practices are considered cutting edge innovations [11], [25]. This notion implies that the main tree provides various roots to begin the search. It is the hub of the main gathering of arbitrary arrangements. The next generation is acquired by evaluating the main assortment according to the root closest to the corn and the level of fineness. The distant roots of the corn are eliminated. The development of bases and services for trees under the ground is highly connected to their root framework. From this perspective, the practices of roots under the ground are considered cutting-edge innovations [5], [11]–[25]. This notion implies that the primary of the tree provides various roots to begin the search. It is the hub for the principal gathering of arbitrary arrangements. The upcoming generation is acquired by assessing the principal assortment in accordance with the root nearest to the corn and the fineness level. The roots that are located far from the corn are eliminated.

The RTO optimization technique is to follow the behavior of the underlying main shaft when searching for groundwater based on the level of control underground. The technique for this calculation is to follow the comportment of the underlying foundation of a tree as it searches for groundwater in accordance with the level of underground control.

On the basis of this principle, inferring another calculation is possible. The factors must be clarified to apply this calculation.

Wetness Degree (Dw): The level of actual wellness between the populace is determined. Moreover, the factors (Rr, Rc, and Rn) are the rates that affect admittance to the arrangement.

The roots of the trees will search for the best arrangement or the closest spot for the beginning of the new populace. The random root (*Rr*) is the nearest to the water. The individuals from the new populace, i.e., the new generation, are from the beginning arrangements proposed [5]. The new populace is determined in accordance with the following:

$$\mathrm{Y}^{\mathrm{new}}(\mathrm{k},\mathrm{i}_{\mathrm{t+1}}) = \mathrm{Y}_{\mathrm{r}}(\mathrm{i}_{\mathrm{t}}) + \mathrm{b}_3.\mathrm{D}_{\mathrm{w}}(\mathrm{k}).\mathrm{randn}.\frac{\mathrm{m}}{\mathrm{t}}. \tag{32}$$

Depending on the choice of the roots closest (*Rn*) to the water, which gather around the damp place, a new generation is created. However, the roots far from moisture are removed. Considering the number of candidates, the following expression is assumed to ascertain the new generation:

$$\mathrm{Y}^{\mathrm{new}}(\mathrm{k},\mathrm{i}_{\mathrm{t+1}}) = \mathrm{Y}^{\mathrm{mei}}(\mathrm{i}_{\mathrm{t}}) + \mathrm{b}_1.\mathrm{D}_{\mathrm{w}}(\mathrm{k}).\mathrm{randn}.\frac{\mathrm{m}}{\mathrm{N}.\mathrm{i}_{\mathrm{t}}}. \tag{33}$$

The new generation is produced by roots that have assembled around the closest place to the water whose root of continuity (*Rc*). A new generation of the population is determined using the following equation:

$$\mathrm{Y}^{\mathrm{new}}(\mathrm{k},\mathrm{i}_{\mathrm{t+1}}) = \mathrm{Y}(\mathrm{k},\mathrm{i}_{\mathrm{t}}) + \mathrm{b}_2.\mathrm{D}_{\mathrm{w}}(\mathrm{k}).\mathrm{randn}. \times \left(\mathrm{Y}^{\mathrm{mei}}(\mathrm{i}_{\mathrm{t}}) - \mathrm{Y}(\mathrm{k},\mathrm{i}_{\mathrm{t}})\right). \tag{34}$$

$$\begin{cases} \tilde{L}_r = \int \dot{\tilde{L}}_r = \int \sqrt{\left(\dfrac{1}{\dot{\tilde{a}}_1}\right)} = \int \sqrt{\left(-\dfrac{1}{\gamma_1 e_\Omega\left(\frac{2pM^2}{3Jv_s}\right)\left(\varphi_{sq}Q_s + \varphi_{sd}P_s\right) - \frac{pM}{J}\varphi_{sq}\varphi_r}\right)}, \\ \tilde{L}_s = \int \dot{\tilde{L}}_s = \int \dfrac{3}{2\dot{\tilde{\sigma}}\dot{\tilde{a}}_5} = \dfrac{3}{2\gamma_5 V_s^2}\int \dfrac{1}{\dot{\tilde{\sigma}}e_{Ps}}. \end{cases} \tag{31}$$

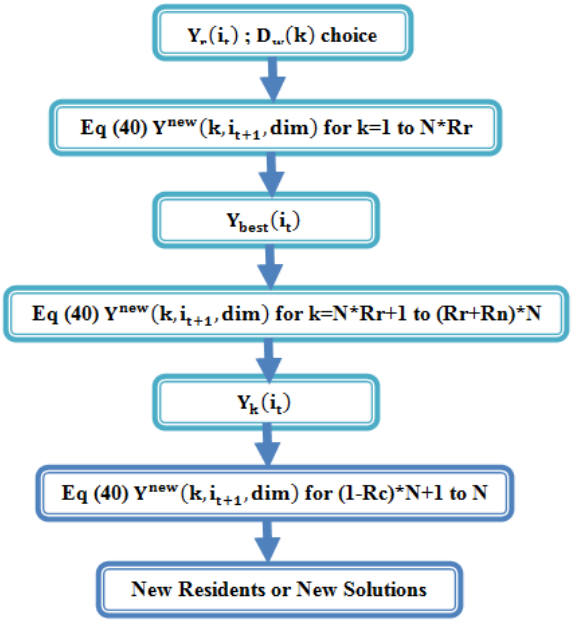

FIGURE 2. Algorithm for Step 3.

A. RTO APPLIED TO THE BACKSTEPPING CONTROL FOR DFIG

The optimal gains of the backstepping algorithm with integral (BSI) in DFIG control is determined through the following steps.

➢ ***Step 1:***

The first generation from the input values for the variables Rr, Rc, and Rn is determined. Knowing that $Rr + Rc + Rn = 100\% = 1$, then the number of candidates N is definite.

➢ ***Step 2:***

From the initial step, we can determine the degree of wetness for the entire primary generation. Then, we assign the control degree (Dw) as shown in Equation (35). At this point, we take the best wetness degree of the generation's members [5].

$$D_w(k) = \begin{cases} \dfrac{f_k}{maxf_k} \text{ for maximal objective} \\ 1 - \dfrac{f_k}{maxf_k} \text{ for minimal objective} \end{cases} \quad (35)$$

➢ ***Step 3:***

➢ ***Step 4:***

If the stop criteria are not met, then return to Step 2.

➢ ***Step 5:***

If the maximum number of iterations is reached, then proceed to Step 6.

➢ ***Step 6:***

The best solution is the individual that provides the optimal values for DFIG control by using the BSI regulator [15].

VI. RESULTS AND DISCUSSION

Figure 6 illustrates the scheme proposed to apply the adaptive nonlinear backstepping control to WECS-DFIG.

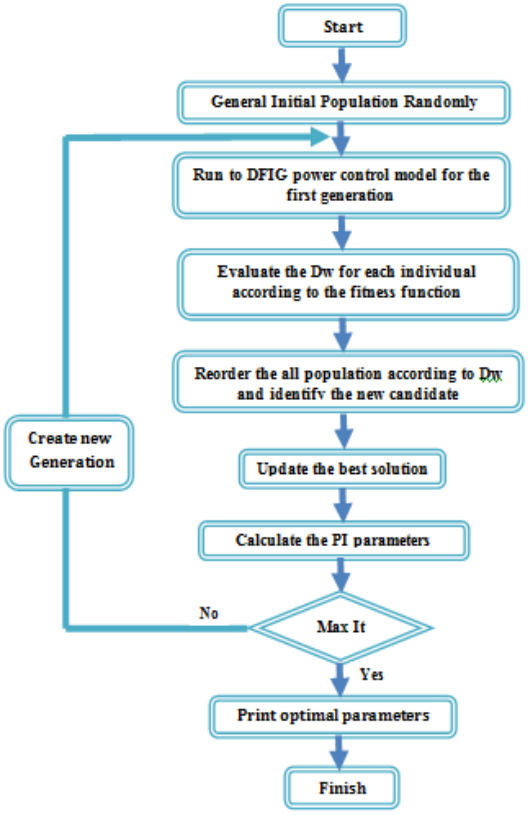

FIGURE 3. Algorithm for RTO.

TABLE 1. RTO parameters.

Parameters	Values
RTO size	20
Maximum number of iterations	20
B_1=b_2=b_3	2
R_n=R_r	0.2
Rc	0.4
Dm	2

The wind system is subjected to a series of simulation tests under the MATLAB/SIMULINK environment to assess the performance, robustness, and stability of the active and reactive power control for DFIG.

The backstepping control technique is developed subsequently on the basis of the adaptive model combined with the RTO technique to improve the robustness and performance of the system.

A. PERFORMANCE TEST

In this section, we focus on analyzing the behavior of DFIG toward the random wind profile. The reactive power is set as zero (Qs_ref = 0 Var) to guarantee a unit power factor and enhance the quality of the energy injected into the electrical grid. The simulations are performed using a real wind profile. The results of the adaptive backstepping control applied to DFIG are presented in Figure 5.

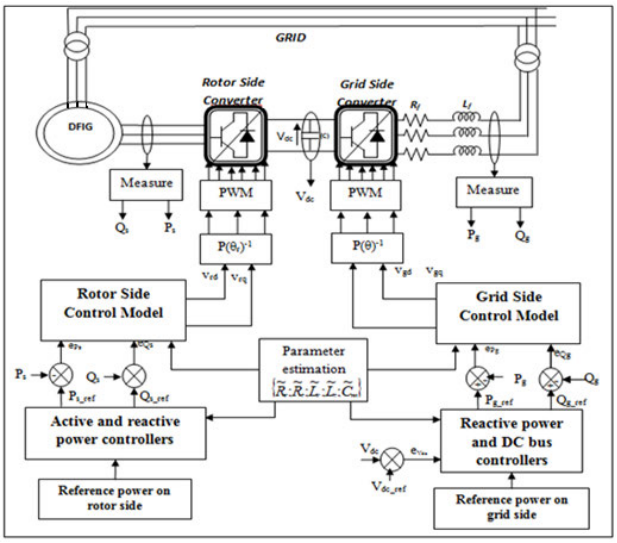

FIGURE 4. Backstepping control applied to DFIG.

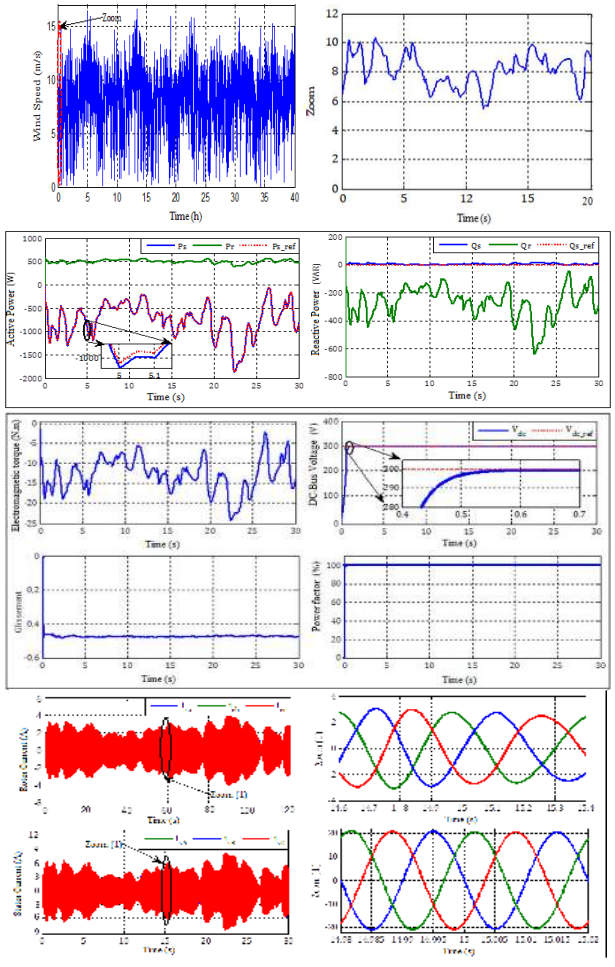

FIGURE 5. Variable wind speed system response.

The winds from the *Dakhla region* located at the south of Morocco are selected.

Figure 5 shows that the active power pursues its reference value generated using the MPPT strategy with a dynamic

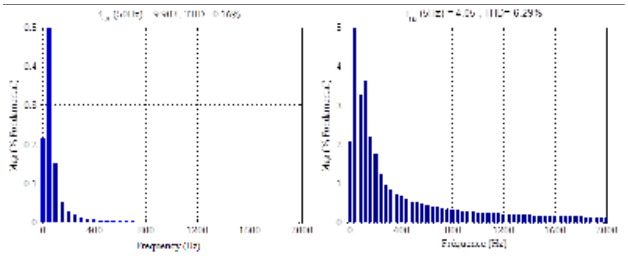

FIGURE 6. Analysis of the harmonics of the current spectra at variable wind speed.

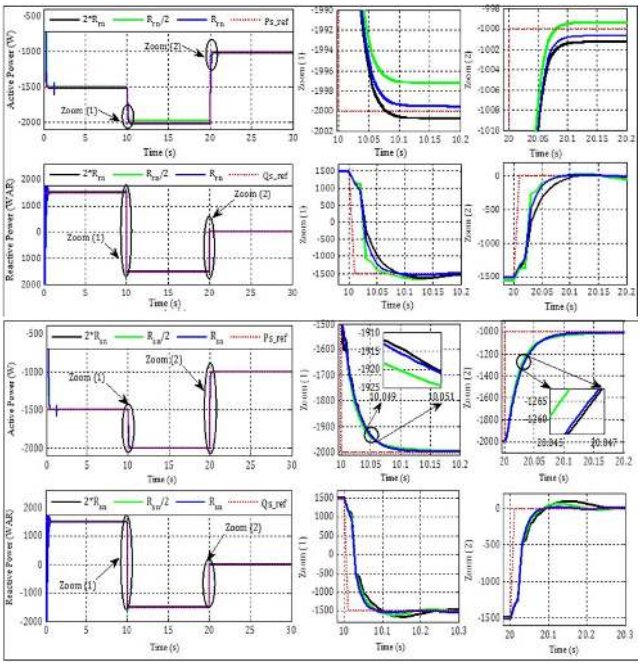

FIGURE 7. Robustness test during resistance variation.

error of $\varepsilon = 1.05\%$. The reactive power always maintains its value (i.e., zero), confirming that the power factor is one under a steady state. The electromagnetic torque of the generator fluctuates following the speed turbine, which reflects wind speed. The power oscillations are insignificant compared with those of the electromagnetic torque. Moreover, the DC link exhibits a fast and precise dynamics, reaching its reference value at $t_{Vdc} = 0.55$ s without overshoot and with a small static error. Stator currents vary with wind variation. Despite the variations in wind, these currents are sinusoidal, with a frequency of 50 Hz. Rotor currents also exhibit the same shape, and their frequency is proportional to mechanical speed. These currents have fewer undulations compared with other techniques.

Figure 6 shows the spectrum of the stator and rotor currents.

THD is clearly 6.29% for the rotor current instead of 0.16% for the stator current in accordance with the IEEE519-2014 [26]–[28] standard.

TABLE 2. Performance comparison.

Publication	Technique	Efficiency	Error	Overshoot	Cosφ	« Robustness »
Zhang, H. B et al. 2011 [17]	Adaptive neural controller	93.5	0.15%	0%	0.997	Moderate–high
	Adaptive fuzzy controller	93.99	0.14%	0%	0.974	Moderate–high
Zemmit, A. et al. 2018 [2]	DTC-classical	92.13	0.32%	5%	0.983	Moderate–high
	DTC-GA-based PI	92.07	0.12%	1%	0.978	Moderate–high
Beltran, B et al. 2008 [10]	Sliding mode	94.82	0.2%	0%	0.972	Low
Proposed technique	Backstepping adaptive	98.99	0,.12%	0%	0.995	High

TABLE 3. DFIG and WT parameters.

DFIG			WT		
Parameters	**Symbol**	**Values**	**Parameters**	**Symbol**	**Values**
Power generator	Ps	1.5 kW	Radius	R	20 m
Stator resistance	Rs	4.85 Ω	Density of air	ρ	1.22 kg/m^3
Rotor resistance	Rr	3.805 Ω	Optimal tip speed ratio	λopt	8
Stator inductance	Ls	274 mH	Maximum power coefficient	Cp	0.45
Rotor inductance	Lr	258 mH			

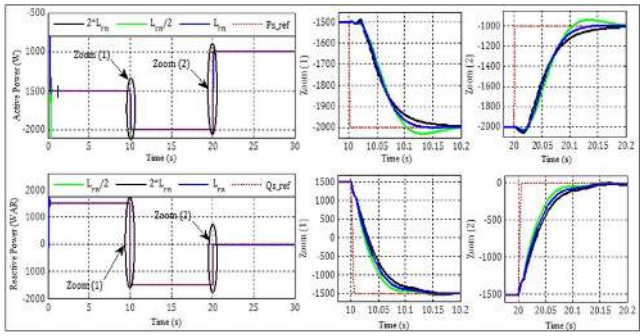

FIGURE 8. Robustness test during inductance variation.

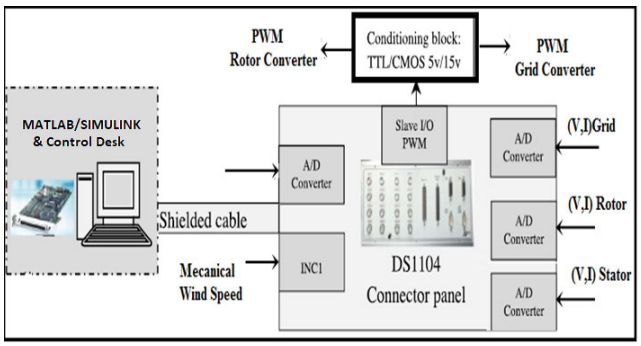

FIGURE 9. dSPACE connection diagram with the wind system.

B. ROBUSTNESS TEST

To check the performance and stability of the adaptive backstepping control in the regulation of the active and reactive powers, several modifications are made at the level of the internal DFIG parameters of the model used.

Various tests are conducted by increasing or decreasing the machine parameters (stator and rotor resistances and inductances). Figures 7 and 8 illustrate the dynamic behavior of the system.

The results show that the active and reactive powers track the imposed references. However, we observe a minor increase in response time due to the changes applied to the stator and rotor resistances (Figure 7). The static error is nearly zero with small ripples. By contrast, the variations in the rotor and stator inductances (Figure 8) generate the same response time and demonstrate low sensitivity during the pursuit of the reference. The decoupling between the active and reactive powers is always ensured. In conclusion, the adaptive backstepping command is robust regardless of the aforementioned parameter variations.

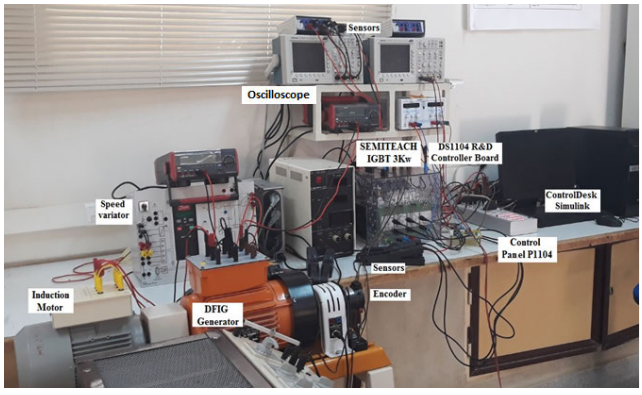

FIGURE 10. Experimental benchmark of the WT system.

VII. EXPERIMENTAL VALIDATION

Before validating the performance of the nonlinear backstepping control on an experimental benchmark, the control algorithm is implemented on a DS1104 R&D control

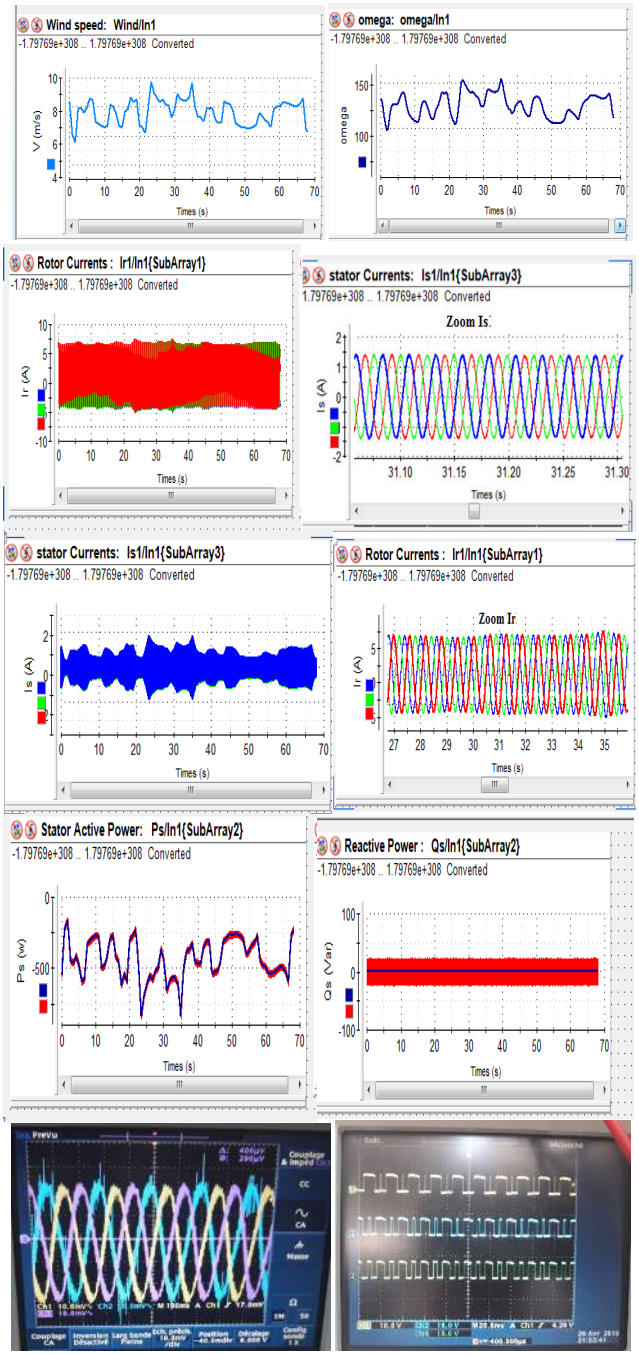

FIGURE 11. Experimental results of the backstepping control applied to WECS.

board developed by dSPACE. The board is linked to a computer via an interface that helps us transfer data between the software and hardware. The hardware of the dSPACE board generates pulse-width modulation (PWM) signals in transistor–transistor logic (TTL) 0/5 V. The software is MATLAB/Simulink, which converts the developed model by using the blocks in the real-time interface (RTI) library that configures the input/output of the system proposed for a real-time algorithm in C language (Figure 9).

Then, the built program source is loaded into the "ControlDesk," and the data acquired to run the system are sent from the sensors and presented graphically.

Figure 10 shows the test-bench for validating the proposed control strategy. This strategy is composed of the following:

- A DFIG **1.5 kW**(the parameters are described in detail in the Appendix)
- An induction motor to drive the DFIG. It plays the role of a turbine and is driven by variable speed from a variable speed drive to generate variable wind speed.
- A Semikron inverter (SEMITEACH IGBT **3 kW**) is connected to the dSPACE board via an isolation and adaptation card.

We select a real wind profile that is generated by a speed controller connected to the DFIG drive motor. Figure 11 presents the results obtained using the adaptive backstepping control.

The obtained results (Figure 11) clearly show good monitoring of active-and-reactive powers with their references. Moreover, mechanical speed gives perfect tracking. The ripples are produced by the fluctuation of wind speed. Reactive power is reasonably low compared with the total generated power. Its value is approximately 20 VAR, which provides a power factor close to one.

Moreover, the stator and rotor currents exhibit a perfect waveform sinusoidal with a frequency of 50 Hz in the stator side and a rapid tracking response. The experimentation results correspond to those obtained in the simulation either in terms of response time or in the wave quality of electrical currents. The adaptive nonlinear backstepping control achieves remarkable results, i.e., shorter response time and good tracking of references.

In summary, the validation results of the backstepping control exhibit good correlation between the experiment and the simulation.

VIII. CONCLUSION

The paper discusses a nonlinear control applied to a WECS-DFIG. The backstepping adaptive control based on the Lyapunov stability technique is proposed to enable the WECS to work in better conditions. To demonstrate the efficiency of the control, we simulate the entire system using a MATLAB/Simulink tool and achieve satisfying results in terms of searches and parameter variations. In the second part, we test the same model on an experimental test bench and implemented it on DS1104. The experimental results achieve the majority of the objectives discussed in the simulation section. The significant findings of this work are as follows.

- ✓ The adaptive-backstepping-control exhibits good performance under a real wind profile.
- ✓ Robustness is ensured using the proposed control algorithm despite variations in the wind profile and machine parameters.
- ✓ The simulation results show that the backstepping control strategy achieves excellent performance when applied to a wind energy conversion system.

✓ The results obtained in practice are close to the simulation results in terms of set-point tracking, robustness, static error, and response time.

In the near future, we will further analyze the dynamic performance of a WECS-DFIG linked to an electrical grid to solve the problems of voltage drop and flickers.

REFERENCES

[1] B. Bossoufi, M. Karim, A. Lagrioui, M. Taoussi, and A. Derouich, "Observer backstepping control of DFIG-generators for wind turbines variable-speed: FPGA-based implementation," *Renew. Energy*, vol. 81, pp. 903–917, Sep. 2015.

[2] A. Zemmit, S. Messalti, and A. Harrag, "A new improved DTC of doubly fed induction machine using GA-based PI controller," *Ain Shams Eng. J.*, vol. 9, no. 4, pp. 1877–1885, Dec. 2018.

[3] E. M. Youness, D. Aziz, E. G. Abdelaziz, B. Jamal, E. O. Najib, Z. Othmane, M. Khalid, and B. Bossoufi, "Implementation and validation of backstepping control for PMSG wind turbine using dSPACE controller board," *Energy Rep.*, vol. 5, pp. 807–821, Nov. 2019.

[4] N. El Ouanjli, A. Derouich, A. El Ghzizal, J. Bouchnaif, Y. El Mourabit, M. Taoussi, and B. Bossoufi, "Real-time implementation in dSPACE of DTC-backstepping for a doubly fed induction motor," *Eur. Phys. J. Plus*, vol. 134, no. 11, pp. 1–14, Nov. 2019.

[5] D. Seyoum, M. F. Rahman, and C. Grantham, "Terminal voltage control of a wind turbine driven isolated induction generator using stator oriented field control," in *Proc. 18th Annu. IEEE Appl. Power Electron. Conf. Expo. (APEC)*, vol. 2, Feb. 2003, pp. 846–852.

[6] B. Bossoufi, M. Karim, A. Lagrioui, M. Taoussi, and M. L. ElHafyani, "Backstepping control of DFIG generators for wide-range variable-speed wind turbines," *Int. J. Automat. Control*, vol. 8, no. 2, pp. 122–140, 2014.

[7] Z. Zhang, Y. Zhao, W. Qiao, and L. Qu, "A space-vector-modulated sensorless direct-torque control for direct-drive PMSG wind turbines," *IEEE Trans. Ind. Appl.*, vol. 50, no. 4, pp. 2331–2341, Jul. 2014.

[8] B. Beltran, M. E. H. Benbouzid, and T. Ahmed-Ali, "Second-order sliding mode control of a doubly fed induction generator driven wind turbine," *IEEE Trans. Energy Convers.*, vol. 27, no. 2, pp. 261–269, Jun. 2012.

[9] B. Yang, T. Yu, H. Shu, J. Dong, and L. Jiang, "Robust sliding-mode control of wind energy conversion systems for optimal power extraction via nonlinear perturbation observers," *Appl. Energy*, vol. 210, pp. 711–723, Jan. 2018.

[10] B. Beltran, T. Ahmed-Ali, and M. Benbouzid, "High-order sliding-mode control of variable-speed wind turbines," *IEEE Trans. Ind. Electron.*, vol. 56, no. 9, pp. 3314–3321, Sep. 2009.

[11] A. Benamor, M. T. Benchouia, K. Srairi, and M. E. H. Benbouzid, "A new rooted tree optimization algorithm for indirect power control of wind turbine based on a doubly-fed induction generator," *ISA Trans.*, vol. 88, pp. 296–306, May 2019.

[12] O. P. Mahela and A. G. Shaik, "Comprehensive overview of grid interfaced wind energy generation systems," *Renew. Sustain. Energy Rev.*, vol. 57, pp. 260–281, May 2016.

[13] I. Matraji, A. Al-Durra, and R. Errouissi, "Design and experimental validation of enhanced adaptive second-order SMC for PMSG-based wind energy conversion system," *Int. J. Electr. Power Energy Syst.*, vol. 103, pp. 21–30, Dec. 2018.

[14] E. Dogan and F. Seker, "The influence of real output, renewable and non-renewable energy, trade and financial development on carbon emissions in the top renewable energy countries," *Renew. Sustain. Energy Rev.*, vol. 60, pp. 1074–1085, Jul. 2016.

[15] J. A. Domínguez-Navarro, R. Dufo-López, J. M. Yusta-Loyo, J. S. Artal-Sevil, and J. L. Bernal-Agustín, "Design of an electric vehicle fast-charging station with integration of renewable energy and storage systems," *Int. J. Electr. Power Energy Syst.*, vol. 105, pp. 46–58, Feb. 2019.

[16] G. Dragomir, A. erban, G. Năstase, and A. I. Brezeanu, "Wind energy in romania: A review from 2009 to 2016," *Renew. Sustain. Energy Rev.*, vol. 64, pp. 129–143, Oct. 2016.

[17] H. B. Zhang, J. Fletcher, N. Greeves, S. J. Finney, and B. W. Williams, "One-power-point operation for variable speed wind/tidal stream turbines with synchronous generators," *IET Renew. Power Gener.*, vol. 5, no. 1, pp. 99–108, 2011.

[18] J. Xie, Y. Wan, B. Wang, S. Fu, K. Lu, and J. H. Kim, "A comprehensive 3-dimensional random mobility modeling framework for airborne networks," *IEEE Access*, vol. 6, pp. 22849–22862, 2018.

[19] D. Granados-Lieberman, R. J. Romero-Troncoso, R. A. Osornio-Rios, A. Garcia-Perez, and E. Cabal-Yepez, "Techniques and methodologies for power quality analysis and disturbances classification in power systems: A review," *IET Generat. Transmiss. Distrib.*, vol. 5, no. 4, pp. 519–529, Apr. 2011.

[20] M. K. Saini and R. Kapoor, "Classification of power quality events—A review," *Int. J. Electr. Power Energy Syst.*, vol. 43, no. 1, pp. 11–19, Dec. 2012.

[21] Y. Han, Y. Feng, P. Yang, L. Xu, Y. Xu, and F. Blaabjerg, "Cause, classification of voltage sag, and voltage sag emulators and applications: A comprehensive overview," *IEEE Access*, vol. 8, pp. 1922–1934, 2020.

[22] S. D. Ahmed, F. S. M. Al-Ismail, M. Shafiullah, F. A. Al-Sulaiman, and I. M. El-Amin, "Grid integration challenges of wind energy: A review," *IEEE Access*, vol. 8, pp. 10857–10878, 2020.

[23] L. Lin, D. Wang, S. Zhao, L. Chen, and N. Huang, "Power quality disturbance feature selection and pattern recognition based on image enhancement techniques," *IEEE Access*, vol. 7, pp. 67889–67904, 2019.

[24] A. A. Abdelsalam, A. A. Salem, E. S. Oda, and A. A. Eldesouky, "Islanding detection of microgrid incorporating inverter based DGs using long short-term memory network," *IEEE Access*, vol. 8, pp. 106471–106486, 2020.

[25] M. M. Islam, E. Hossain, S. Padmanaban, and C. W. Brice, "A new perspective of wind power grid codes under unbalanced and distorted grid conditions," *IEEE Access*, vol. 8, pp. 15931–15944, 2020.

[26] G. S. Chawda, A. G. Shaik, O. P. Mahela, S. Padmanaban, and J. B. Holm-Nielsen, "Comprehensive review of distributed FACTS control algorithms for power quality enhancement in utility grid with renewable energy penetration," *IEEE Access*, vol. 8, pp. 107614–107634, 2020.

[27] F. Allella, E. Chiodo, G. M. Giannuzzi, D. Lauria, and F. Mottola, "On-line estimation assessment of power systems inertia with high penetration of renewable generation," *IEEE Access*, vol. 8, pp. 62689–62697, 2020.

[28] T. Zhong, S. Zhang, G. Cai, Y. Li, B. Yang, and Y. Chen, "Power quality disturbance recognition based on multiresolution S-transform and decision tree," *IEEE Access*, vol. 7, pp. 88380–88392, 2019.

BADRE BOSSOUFI (Graduate Student Member, IEEE) was born in Fez, Morocco, in 1985. He received the Ph.D. degree in electrical engineering from the Faculty of Sciences, Sidi Mohammed Ben Abdellah University, Fez, Morocco, and the Ph.D. degree from the Faculty of Electronics and Computer, The University of Pitesti, Romania, and the Department of Electrical Engineering, Montefiore Institute, Liège, Belgium, in 2012.

He was a Professor of Electrical Engineering with the Faculty of Sciences, Sidi Mohamed Ben Abdellah University. His research interests include static converters, electrical motor drives, power electronics, smart grid, renewable energy, and artificial intelligent.

MOHAMMED KARIM was born in Fez, Morocco. He is currently a Professor of Computer Science and Electronics with the Faculty of Sciences, Sidi Mohamed Ben Abdellah University, Fez. He is also the Head of the STIC Research Group and the ISAI Master. He is the Chairman of the Organization Committee of a series of workshops and conferences. He is working on different projects, such as computer vision, biomedical engineering, and E-learning.

MOHAMMED TAOUSSI was born in Fez city, Morocco. He received the master's degree in industrial electronics from the Faculty of Sciences-Fez, in 2013. He is a Professor of Faculty of Sciences, University Sidi Mohammed Ben Abdellah, Morocco, where he is currently pursuing the Ph.D. degree in electrical engineering. His research interests include static converters, electrical motor drives, and power electronics, smart grid, renewable energy and artificial intelligence.

HALA ALAMI AROUSSI received the M.S. degree in industrial automated systems engineering from Sidi Mohammed Ben Abdellah University, Fez, Morocco. She is currently pursuing the Ph.D. degree in electrical engineering–renewable energy with Mohamed Premier University, Oujda, Morocco. She is a member of the Laboratory of Electrical Engineering and Maintenance (LGEM). Her research interests include modeling, control of wind energy conversion systems applied to a doubly fed induction machine using DSPACE.

MANALE BOUDERBALA received the master's degree in engineering of industrial automated systems from the Faculty of Sciences Dhar el Mahrez Fez, Sidi Mohammed Ben Abdellah University, Fez, Morocco, where she is currently pursuing the Ph.D. degree in electrical engineering. She is a member of the LISTA Laboratory. Her research interests include renewable energy, static converters, electrical motor drives, and power electronics.

OLIVIER DEBLECKER was born in 1971. He received the civil electrical engineering and Ph.D. degrees in electrical engineering from the Faculté Polytechnique de Mons, Mons, Belgium, in 1995 and 2001, respectively. He is currently an Assistant Professor with the Electrical Engineering Division, Faculté Polytechnique de Mons. His research interests include magnetic fields calculation using numerical methods, hysteresis modeling, and power electronics. He has been a member of the Belgian Royal Society of Electrical Engineers (SRBE/KBVE), since 1996, and the European Power Electronics and Drives (EPE) Association, since 2004.

SAAD MOTAHHIR (Member, IEEE) received the Engineering degree in embedded system from ENSA, Fez, Morocco, in 2014, and the Ph.D. degree in electrical engineering from SMBA University, in 2018. From 2014 to 2019, he was an Embedded System Engineer with Zodiac Aerospace, Morocco. Since 2019, he has been a Professor with ENSA, SMBA University, Fez. He has published a good number of papers in journals and conferences in the last few years, most of which are related to photovoltaic (PV) solar energy and embedded systems. He published number of patents in Morocco patent office. He edited a springer book and acted as a Guest Editor of different special issues and topical collections. He is a Reviewer and the Editorial Board of different journals. He was associated with more than 30 international conferences as a Program Committee/Advisory Board/Review Board Member.

ANAND NAYYAR received the Ph.D. degree in computer science from Desh Bhagat University, in 2017, in the area of wireless sensor networks and Swarm intelligence. He is currently working with the Graduate School, Duy Tan University, Da Nang, Vietnam. A Certified Professional with more than 75 Professional certificates from CISCO, Microsoft, Oracle, Google, Beingcert, EXIN, GAQM, Cyberoam, and so on. He is currently working in the area of wireless sensor networks, MANETS, Swarm intelligence, cloud computing, the Internet of Things, blockchain, machine learning, deep learning, cyber security, network simulation, and wireless communications. He has authored/coauthored cum edited more than 25 Books of Computer Science. He associated with more than 500 International Conferences as a Programme Committee/Chair/Advisory Board/Review Board Member. He has five Australian Patents to his credit in the area of Wireless Communications, Artificial Intelligence, IoT, and Image Processing. He published more than 450 research papers in various National and International Conferences, International Journals (Scopus/SCI/SCIE/SSCI Indexed) with High Impact Factor. He is a member of more than 50 Associations as a Senior Member and a Life Member. He is also acting as the ACM Distinguished Speaker. He received more than 30 Awards for Teaching and Research—Young Scientist Award, the Best Scientist Award, the Young Researcher Award, the Outstanding Researcher Award, Excellence in Teaching and many more. He is acting as an Associate Editor for *Wireless Networks* (Springer), IJDST, IJISP, and IJCINI. He is acting as the Editor-in-Chief of IGI-Global, USA, Journal titled *International Journal of Smart Vehicles and Smart Transportation* (IJSVST).

MOHAMMED A. ALZAIN received the bachelor's degree in computer science from King Abdulaziz University, Saudi Arabia, in 2004, and the master's degree in information technology from La Trobe University, in 2010. He is currently pursuing the Ph.D. degree with the Department of Computer Science and Computer Engineering, La Trobe University, Melbourne, VIC, Australia. He is a Ph.D. Research in cloud computing security under the Supervision of Assoc/Prof. Ben Soh and Dr. Eric Pardede. He is also a Lecturer with the Faculty of Computer Science and Information Technology, Al Taif University, Saudi Arabia. His areas of research interests include cloud computing security, distributed systems, and database as a service.